

Supporting Information

Temperature-triggered triplex bistable switch in a hybrid multifunctional material: $[(\text{CH}_2)_4\text{N}(\text{CH}_2)_4]_2[\text{MnBr}_4]$

Li Xu,^a Ji-Xing Gao,^a Xiao-Gang Chen,^a Xiu-Ni Hua^a and Wei-Qiang Liao^{*ab}

^aOrdered Matter Science Research Center, Jiangsu Key Laboratory for Science and Applications of Molecular Ferroelectrics, College of Chemistry and Chemical Engineering, Southeast University, Nanjing 211189, P. R. China

^bOrdered Matter Science Research Center, College of Chemistry, Nanchang University, Nanchang 330031, P. R. China

*E-mail: weiqiangliao@seu.edu.cn

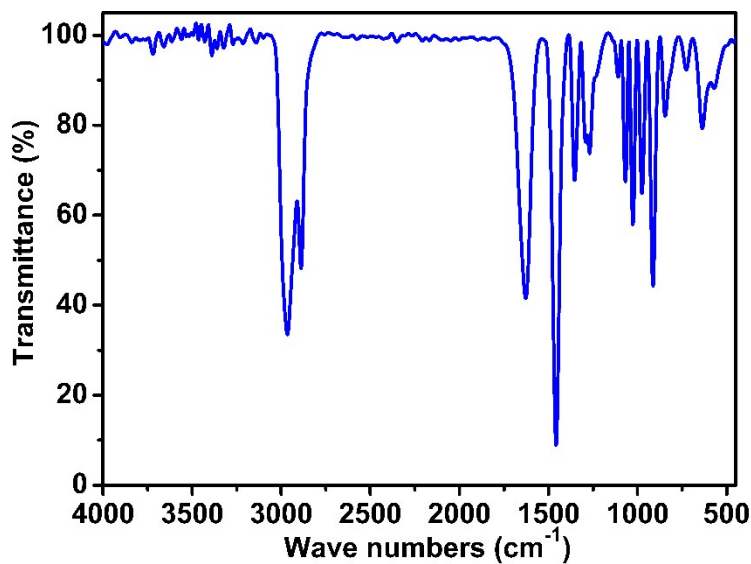


Fig. S1 The IR spectrum of **1** in KBr pellet, recorded on a Shimadzu model IR-60 spectrometer at room temperature.

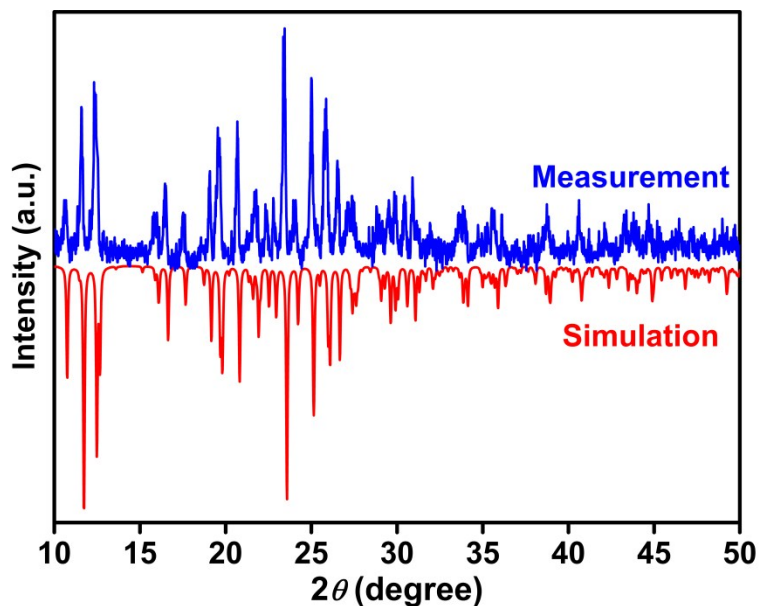


Fig. S2 The PXRD pattern of **1** measured at room temperature (blue line) matches well with the simulated one (red line) based on the single crystal structure, indicating the purity of the phase.

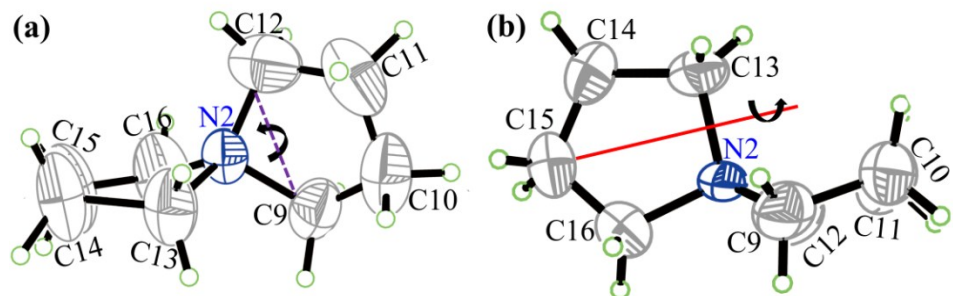


Fig. S3 (a) Projection of the asymmetric unit of the spirocyclic ammonium cation in crystal of **1** in the envelop conformation. Purple dotted line represents the folding line. (b) Projection of the asymmetric unit of the same spirocyclic ammonium cation in the twist conformation along the twist axis (red line) with atomic numbering (ORTEP, 30% probability ellipsoids, hydrogen atoms with arbitrary radii).

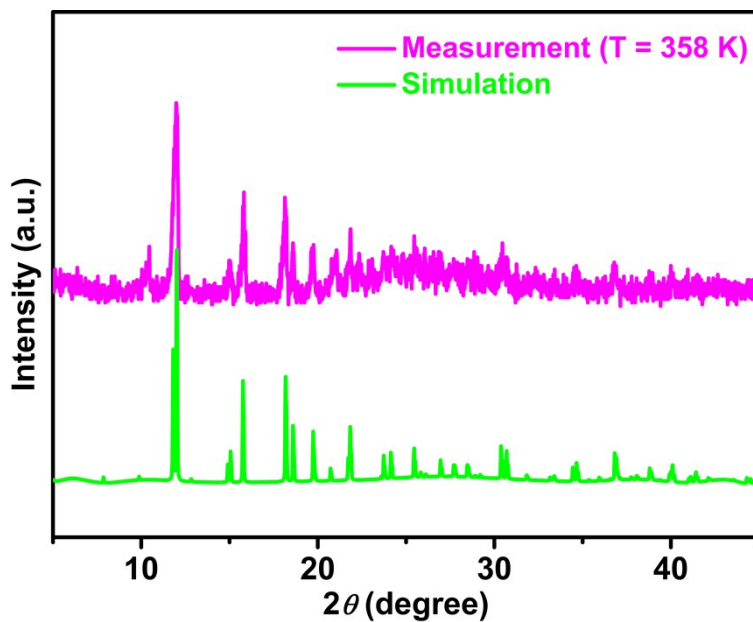


Fig. S4 Pawley refinement of PXRD data of **1** collected at 358 K, revealing a tetragonal lattice with $a = b = 9.9547(8)$ Å, $c = 24.4711(2)$ Å with one of the most possible space group of $P4_12_12$.

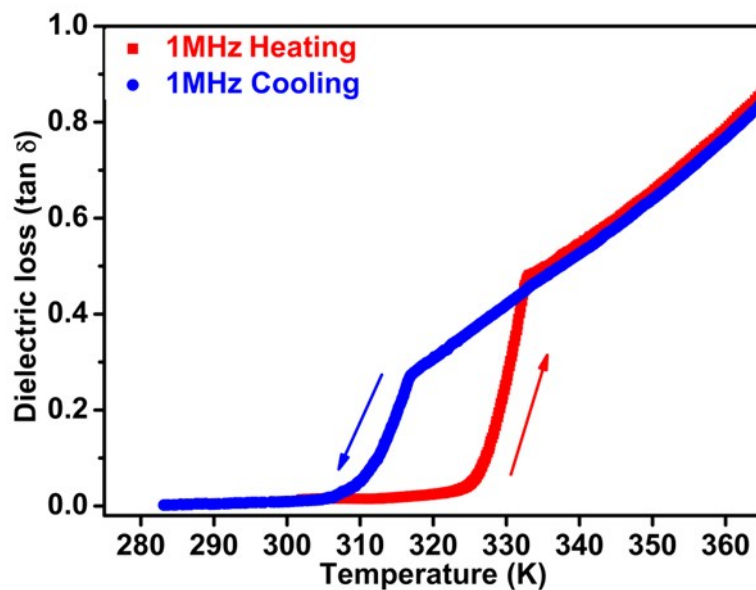


Fig. S5 Dielectric loss ($\tan \delta$) of the dielectric permittivity of compound **1** measured on a power sample in the heating–cooling cycles at 1 MHz.

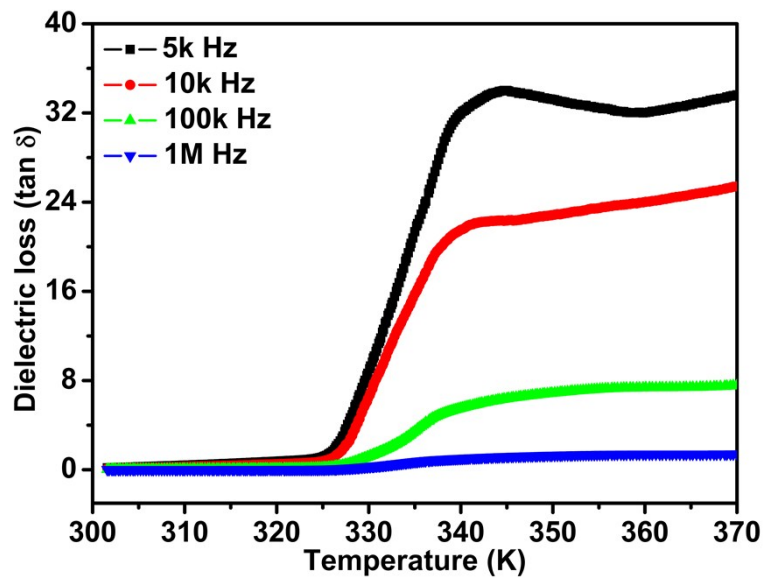


Fig. S6 The dielectric loss ($\tan \delta$) of compound 1 under different frequencies (5k-1MHz) upon heating process.

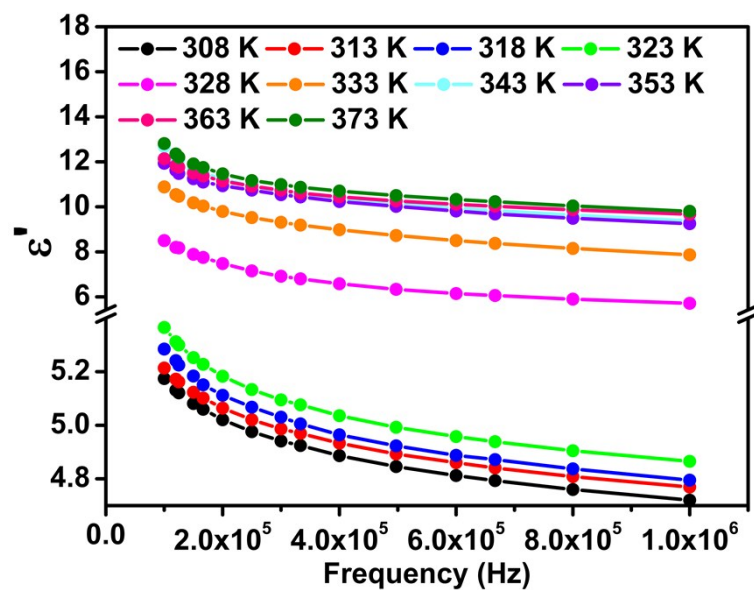


Fig. S7 Frequency dependence of ϵ' values for compound 1 in the temperature ranges of 308-373 K.

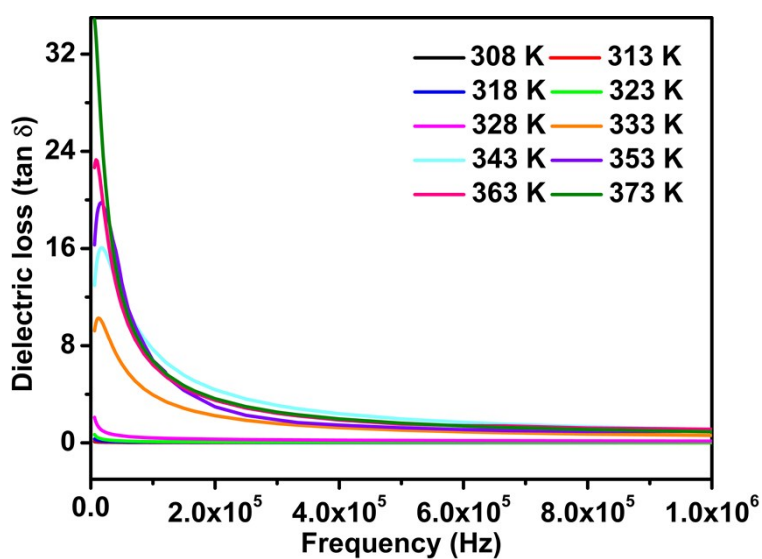


Fig. S8 Frequency dependence of the dielectric loss ($\tan \delta$) of **1** obtained at various temperatures (308 K-373 K).

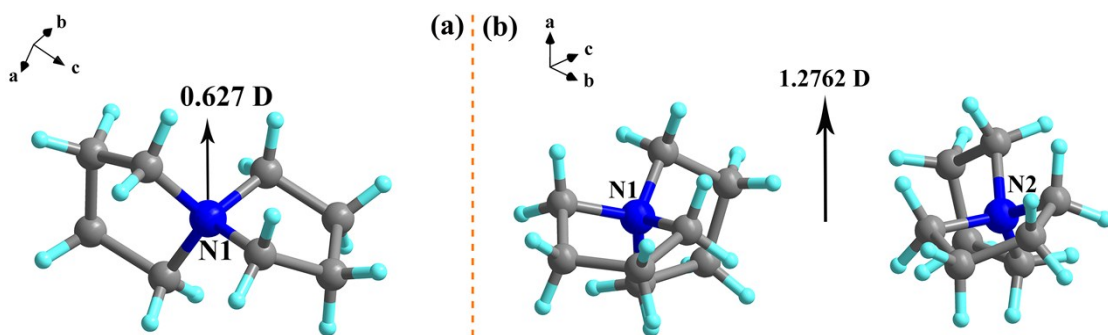


Fig. S9 The dipole moment direction and magnitude of cation A (a) and two cations (b) of **1** at LTP calculated through GaussView 5.0.9 software.

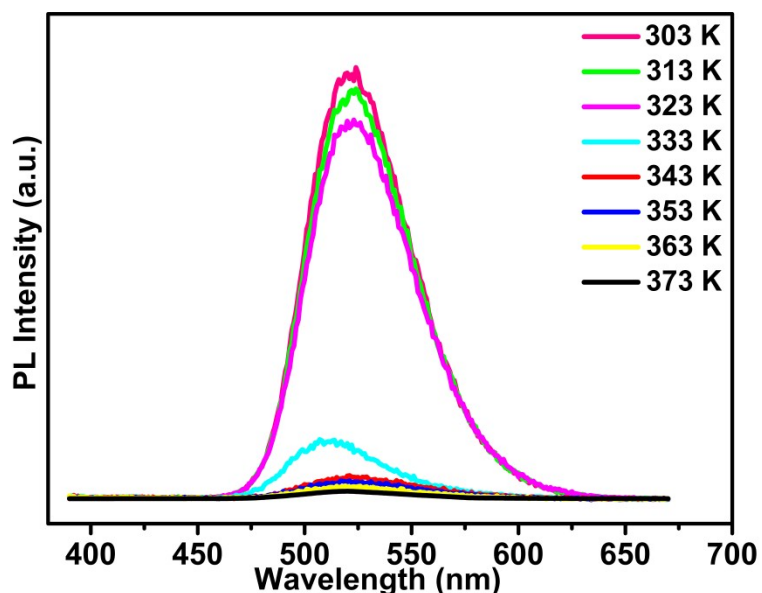


Fig. S10 Variable-temperature emission spectra of **1** under 360 nm excitation.

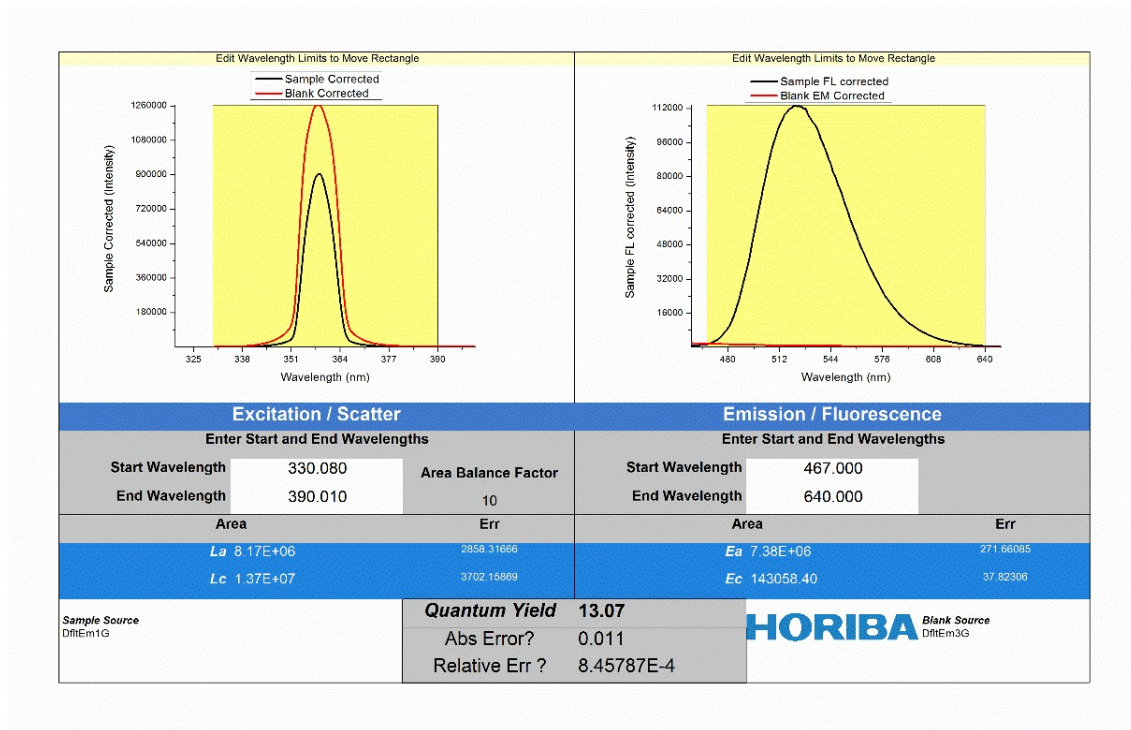


Fig. S11 The quantum yield measurement of **1**, giving a quantum yield of 13.07%.

Table S1. Crystallographic data and structure refinements of **1** at 293 K

Empirical formula	(C ₈ H ₁₆ N) ₂ MnBr ₄
Formula weight	626.98
Temperature/K	293
Crystal system	Orthorhombic
Space group	<i>P</i> 2 ₁ 2 ₁ 2 ₁
a/Å	9.2541(4)
b/Å	13.9651(6)
c/Å	17.9090(9)
α/deg	90.00
β/deg	90.00
γ/deg	90.00
Volume /Å ³	2314.46(18)
Z, density/(g·cm ⁻³)	4, 1.799
<i>F</i> (000)	1228
Collected reflections	4054
Unique reflections	2843
Parameters refined	208
<i>R</i> ₁ [<i>I</i> >2σ(<i>I</i>)]	0.051

wR_2 [$I > 2\sigma(I)$]	0.124
GOF	1.02

Table S2. The key bond lengths [Å] and angles [°] for **1** at 293 K

Br1—Mn1	2.4985 (11)	C7—C8	1.447 (12)
Br2—Mn1	2.5043 (11)	C8—N1	1.523 (8)
Br3—Mn1	2.5158 (10)	C9—N2	1.496 (11)
Br4—Mn1	2.5095 (11)	C9—C10	1.519 (14)
C1—N1	1.478 (10)	C10—C11	1.425 (19)
C1—C2	1.496 (12)	C11—C12	1.482 (16)
C2—C3	1.488 (13)	C12—N2	1.437 (11)
C3—C4	1.555 (12)	C13—N2	1.500 (11)
C4—N1	1.494 (8)	C13—C14	1.528 (13)
C5—N1	1.494 (10)	C14—C15	1.429 (13)
C5—C6	1.511 (13)	C15—C16	1.430 (12)
C6—C7	1.453 (13)	C16—N2	1.469 (11)
N1—C1—C2	103.2 (7)	Br1—Mn1—Br4	109.73 (4)
C3—C2—C1	104.4 (7)	Br2—Mn1—Br4	108.55 (4)
C2—C3—C4	106.8 (7)	Br1—Mn1—Br3	107.95 (4)
N1—C4—C3	103.1 (6)	Br2—Mn1—Br3	106.77 (4)
N1—C5—C6	101.1 (6)	Br4—Mn1—Br3	112.18 (4)
C7—C6—C5	108.2 (8)	C1—N1—C5	111.9 (6)
C8—C7—C6	106.6 (7)	C1—N1—C4	104.8 (6)
C7—C8—N1	106.2 (6)	C5—N1—C4	114.4 (6)
N2—C9—C10	102.5 (8)	C1—N1—C8	112.1 (6)
C11—C10—C9	104.8 (9)	C5—N1—C8	102.4 (5)
C10—C11—C12	106.2 (10)	C4—N1—C8	111.4 (5)
N2—C12—C11	104.9 (9)	C12—N2—C16	120.2 (8)
N2—C13—C14	102.8 (7)	C12—N2—C9	98.8 (7)
C15—C14—C13	105.8 (8)	C16—N2—C9	104.2 (7)
C14—C15—C16	109.4 (8)	C12—N2—C13	117.8 (8)

C15—C16—N2	108.0 (8)	C16—N2—C13	104.2 (7)
Br1—Mn1—Br2	111.65 (4)	C9—N2—C13	110.6 (7)

Table S3. Hydrogen-Bond Geometry (\AA , deg) for C-H \cdots Br interactions at 293 K in **1**

$D\text{—H}\cdots A$	$D\text{—H}$	$H\cdots A$	$D\cdots A$	$\angle D\text{—H}\cdots A$
C14—H14A \cdots Br1	0.97	2.91	3.828 (12)	159
C8—H8A \cdots Br2	0.97	2.96	3.834 (7)	151
C1—H1A \cdots Br3	0.97	3.02	3.910 (8)	153
C8—H8B \cdots Br3	0.97	3.04	3.907 (8)	149
C1—H1B \cdots Br4	0.97	3.00	3.815 (8)	142